New Journal of Physics
The open access journal at the forefront of physics

Deutsche Physikalische Gesellschaft DPG IOP Institute of Physics

PAPER • OPEN ACCESS

Experimental verification of ‘waveguide’ plasmonics

To cite this article: Filipa R Prudêncio *et al* 2017 *New J. Phys.* **19** 123017

New Journal of Physics
The open access journal at the forefront of physics

Deutsche Physikalische Gesellschaft DPG
IOP Institute of Physics

Published in partnership with: Deutsche Physikalische Gesellschaft and the Institute of Physics

OPEN ACCESS

RECEIVED
8 June 2017

REVISED
3 October 2017

ACCEPTED FOR PUBLICATION
13 October 2017

PUBLISHED
6 December 2017

PAPER

Experimental verification of 'waveguide' plasmonics

Filipa R Prudêncio[1,2], **Jorge R Costa**[1,2], **Carlos A Fernandes**[1], **Nader Engheta**[3] and **Mário G Silveirinha**[1]

[1] University of Lisbon—Instituto Superior Técnico and Instituto de Telecomunicações, Avenida Rovisco Pais 1, 1049-001 Lisboa, Portugal
[2] Instituto Universitário de Lisboa (ISCTE-IUL), Lisboa, Portugal
[3] University of Pennsylvania, Department of Electrical and Systems Engineering, Philadelphia, PA 19104, United States of America

E-mail: filipa.prudencio@lx.it.pt

Keywords: metamaterials, plasmonics, surface plasmons polaritons

Abstract

Surface plasmons polaritons are collective excitations of an electron gas that occur at an interface between negative-ε and positive-ε media. Here, we report the experimental observation of such surface waves using simple waveguide metamaterials filled only with available positive-ε media at microwave frequencies. In contrast to optical designs, in our setup the propagation length of the surface plasmons can be rather long as low loss conventional dielectrics are chosen to avoid typical losses from negative-ε media. Plasmonic phenomena have potential applications in enhancing light–matter interactions, implementing nanoscale photonic circuits and integrated photonics.

1. Introduction

Surface plasmon polaritons (SPPs) are guided electromagnetic waves at the interface between two materials where the real part of the permittivity changes its sign across the interface [1, 2]. Negative permittivity media are the key components in the exciting field of plasmonics and metamaterials [1–5], although they typically do suffer from strong losses. Negative permittivity materials can be artificially synthesized, for instance, by considering a regular array of conducting wires [6–9] or metallic waveguide structures [10–15]. In particular, several studies use the equivalence between an effective permittivity and a single structural mode propagating in a parallel-plate waveguide. Structural dispersion plays an important role in this context and the resulting effective permittivity depends on the filling material, operating frequency and on the distance between the metallic plates [11]. Furthermore, in [16] it is demonstrated that a waveguide with split ring resonators can mimic a medium with simultaneously negative permittivity and permeability [17] for transverse electric (TE) modes propagating inside the structure. A dual analysis has been presented in [18] for the case of transverse magnetic (TM) modes. Other structures have been put forward to imitate the confinement characteristic of surface plasmons at microwaves [19–22].

While the realization of artificial media with negative-ε response in the bulk is well established in the literature, at abrupt interfaces the typical metamaterial response typically deviates considerably from that of an ideal continuum mainly due to spatial dispersion effects and subsequent undesirable mode coupling [23–25]. Thus, most metamaterial designs fail to imitate some of the salient and interesting features of SPPs in metal nanostructures at optics. A solution to overcome this limitation was reported in [10], wherein Giovampaola and Engheta have put forward a parallel-plate waveguide design for an effective negative-ε medium that retains the plasmonic features at material interfaces, even though the waveguide is filled with only positive-epsilon materials. The crucial novelty of that design is the insertion of tiny metallic wires at the interface between the two regions, preventing unwanted coupling from the TE_1 to TM_1 modes, and thus guaranteeing in this manner the exclusive propagation of the TE_1 mode and the suppression of spatially dispersive effects [23–25]. The parallel-plate waveguide in [10] has two regions with two different positive-ε dielectrics, avoiding the dissipative losses from conventional negative-ε media (e.g., metals at optical frequencies). Building on this idea, the concept of waveguide metatronics was introduced in [26].

Here, relying on the design of [10], we report an experimental verification of single-interface 'microwave plasmons' using waveguide structures without negative-ε media. We recently learned that the effective SPP

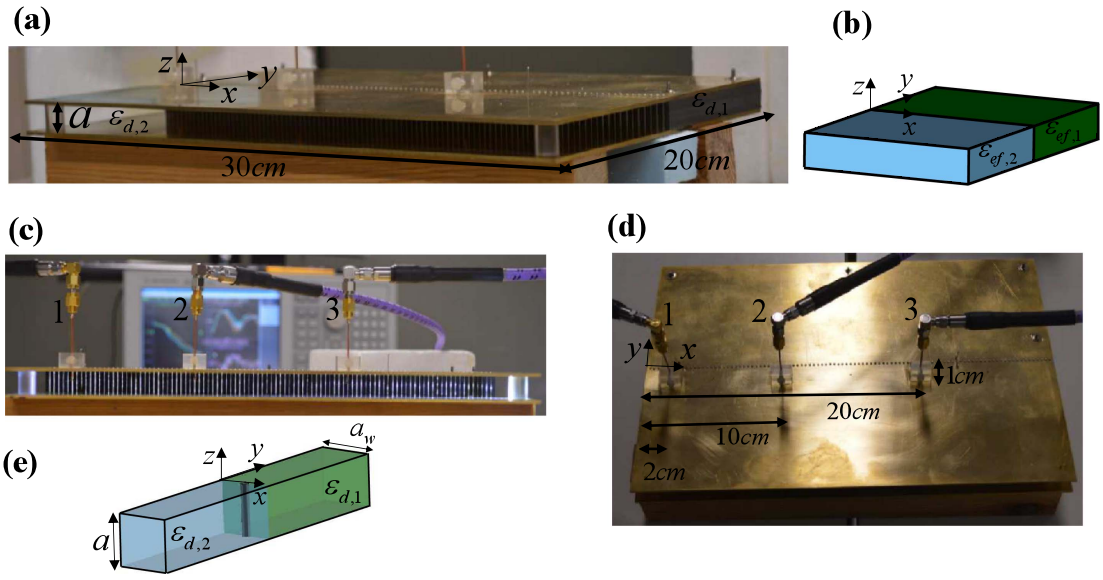

Figure 1. (a) Photograph of the parallel-plate–metamaterial waveguide filled with two dielectrics with positive permittivities, $\varepsilon_{d,1}$ and $\varepsilon_{d,2}$. The distance between the metallic plates is a. (b) Effective medium model of the structure: two materials with equivalent permittivities, $\varepsilon_{\mathrm{ef},1}$ and $\varepsilon_{\mathrm{ef},2}$, are separated by a planar interface. (c) Front view of our structure, showing the thin metallic wires that suppress the excitation of TM modes at the interface. (d) Top view of the structure. The dipole antennas are inserted at a distance $x = 2$ cm, and $x = 10$ cm and $x = 20$ cm from the sidewall. (e) Unit cell of the equivalent periodic structure formed by two half-spaces filled by materials with permittivities, $\varepsilon_{d,1}$ and $\varepsilon_{d,2}$, and a single wire at the interface (the top and bottom metallic walls are not shown). The period of the structure along the x-direction is $a_w = 3$ mm.

propagation in a closed waveguide environment was also studied in [27], but in contrast with our work, in [27] the plasmons are supported by multiple interfaces. To the best of our knowledge, here we present the first experimental verification of a plasmonic-type waveguide (formed by only good metals and regular dielectrics) that supports *single interface modes*. Note that other guides proposed in the literature (e.g. [19–21]) to imitate SPPs at microwaves typically consist of a periodic array of grooves with a depth on the order of one quarter of wavelength, and hence the guided wave is not truly localized at the interface. In contrast our solution truly emulates the ultra-subwavelength confinement characteristic of SPPs.

2. Theory and experimental results

A photo of our waveguide-metamaterial prototype is shown in figure 1(a). It consists of a standard parallel-plate waveguide filled with two different dielectrics with positive permittivities $\varepsilon_{d,1}$ and $\varepsilon_{d,2}$. The metal plates with area 20 cm $\times$ 30 cm are made of brass and are separated by distance $a = 1.29$ cm. The region $y > 0$ is filled by a stack of eight glued 1.57 mm thick RT/duroid® 5880 dielectric slabs, with complex permittivity $\varepsilon_{d,1} = 2.2(1 + \mathrm{i}\tan\delta)$ and loss tangent $\tan\delta = 9 \times 10^{-4}$. The waveguide region $y < 0$ is simply filled with air ($\varepsilon_{d,2} = 1$). About 100 vertical thin metallic pins with radius $r_w = 0.3$ mm were inserted along the interface ($y = 0$) of the two regions through holes drilled in the metallic plates. The distance between adjacent pins is $a_w = 3$ mm. The metallic pins fit tightly through the holes, ensuring a good ohmic contact with the metallic plates. The metallic pins prevent mode coupling between the transverse electromagnetic (TEM), TE_1, and TM_1 modes, and are absolutely essential to reproduce the relevant plasmonic phenomena. Indeed, the relevant mode of operation of the system has a horizontal polarization (TE_1 mode), i.e., the electric field is parallel to the metallic plates. However, at the interface of the two dielectric regions there is the possibility of exciting a wave with an undesired (vertical) polarization. The role of the metallic pins is precisely to prevent the excitation of this wave, and ensure in this manner that our system really mimics a plasmonic waveguide.

The analogy between the propagation of the TE_1 mode (with electric field parallel to the metallic plates) and an effective medium [11] leads to the corresponding relative effective permittivity $\varepsilon_{\mathrm{ef}}$, which depends on the radian frequency $\omega = 2\pi f$, the dielectric constant of the filling material, ε_d, and the separation between the parallel metallic plates a as:

$$\varepsilon_{\mathrm{ef}} = \varepsilon_d - \left(\frac{\pi c}{\omega a}\right)^2, \tag{1}$$

where c is the speed of light in vacuum. Thus, from an effective medium perspective, this waveguide structure simply provides two dispersive materials joint at the interface, as schematically depicted in figure 1(b). For our

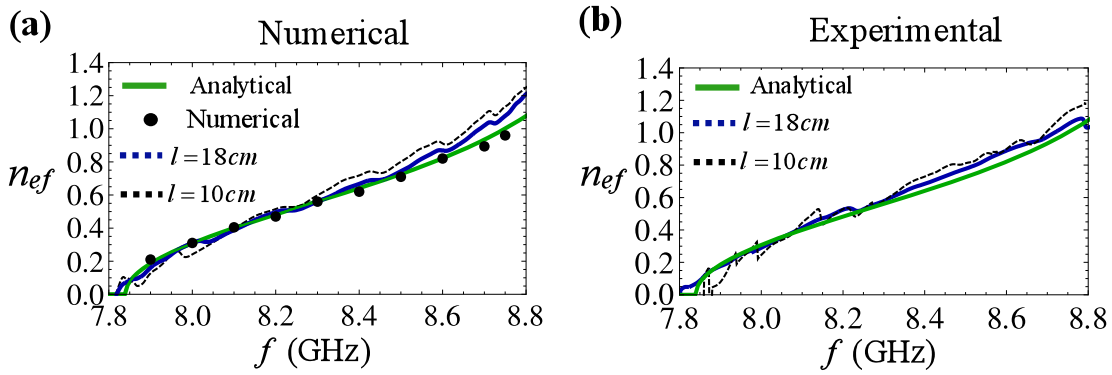

Figure 2. (a), (b) Dispersion diagrams of the single interface SPP modes supported by our plasmonic waveguide-metamaterial (figure 1(a)). Solid green line: analytical result calculated with equation (2). (a) Simulations obtained with the CST Microwave Studio® [28]. Discrete circle symbols: 'exact' dispersion diagram numerically calculated using the Bloch-boundary conditions. Blue dashed curve: dispersion diagram extracted from the phase of the numerically calculated S_{31} parameter for a propagating distance $l = 18$ cm. Dotted black curve: dispersion diagram extracted from the phase of the numerically calculated S_{32} parameter for a propagating distance $l = 10$ cm. (b) Experimental results obtained from the measured scattering parameters, S_{31} and S_{32}, for a distance between ports, $l = 18$ cm and $l = 10$ cm, respectively.

design, following equation (1), the equivalent plasma frequencies—wherein the real part of the effective permittivity changes sign—for the regions 1 ($y > 0$) and 2 ($y < 0$) are 7.84 GHz and 11.62 GHz, respectively, and correspond to the cut-off frequencies of the TE_1 mode.

Therefore, in the frequency interval 7.84 GHz $< f <$ 11.62 GHz our structure is expected to mimic effectively an interface between positive-ε and negative-ε materials. For example, for the operating frequency 8.8 GHz, the effective permittivities are $\varepsilon_{ef,1} = 0.45$ and $\varepsilon_{ef,2} = -0.75$. As is well-known, an interface between two media with $\varepsilon_{ef,1}\varepsilon_{ef,2} < 0$ may support SPP waves with a guided propagation constant β_g given as [2]:

$$\frac{\beta_g}{k_0} \equiv n_{ef} = \sqrt{\frac{\varepsilon_{ef,1}\varepsilon_{ef,2}}{\varepsilon_{ef,1} + \varepsilon_{ef,2}}}, \tag{2}$$

where $k_0 = \omega/c$ is the free-space wave number and $n_{ef} = n'_{ef} + in''_{ef}$ is the guided effective refractive index. The guided wavelength is related to the vacuum wavelength as $\lambda_g = \lambda_0/n'_{ef}$. The SPP resonance, wherein $\varepsilon_{ef,1} + \varepsilon_{ef,2} = 0$, occurs at 9.19 GHz. The propagation length of the SPPs can be estimated as $(\lambda_g/2\pi)\,n'_{ef}/n''_{ef}$ where $n'_{ef}/n''_{ef} \approx 200$ is roughly determined from the loss tangent of the dielectric ($n'_{ef}/n''_{ef} \sim 1/\tan\delta$). In this frequency range the factor n'_{ef}/n''_{ef} is at least one order of magnitude larger than in optics. In the appendix, we provide a detailed study of the effect of dielectric and metal loss and demonstrate that it is negligible for microwave designs.

We computed the 'exact' dispersion diagram of the proposed single-interface metamaterial waveguide using the frequency domain solver of CST Microwave Studio® [28] considering a single unit cell of the structure (see figure 1(e)) and Bloch boundary conditions along the x-direction. The dispersion diagram obtained with the CST Microwave Studio® is represented in figure 2(a) with discrete symbols (black circles) and is superimposed on the theoretical result (2) (solid green line). As seen, there is a remarkable agreement between the numerical and analytical results, further validating the theory of [10].

In order to determine experimentally the dispersion of the SPPs, the structure was excited by a horizontal dipole with arms aligned along the x-direction. The excitation dipole is either at port 1 or at port 2 of figure 1(d), depending on the measurement. The guided wave is characterized using a similar receiving antenna (port 3) (see figures 1(c) and (d)). The dipole can excite both a space wave and the guided SPP mode, the latter being the main radiation channel. Indeed, the efficiency of the excitation depends on how well the fields generated by the dipole match the profile of a mode. Importantly, the near-field of the dipole is formed by high-frequency spatial harmonics which can strongly couple to the SPP mode due to its intrinsic short wavelengths.

Neglecting the effects of reflections of the SPP wave at the receiving antenna and at the sidewalls (all the lateral walls were covered with microwave absorbers), it follows that the phase ϕ of the transmission coefficient (scattering parameter S_{ij}) from port j to port i is such that $\phi = \beta_g l + \phi_0$, where l is the distance between the two ports and ϕ_0 is some reference phase that only depends on the properties of the dipole antennas. Hence, the effective refractive index of the SPP surface wave $n_{ef} = \beta_g/k_0$ may be obtained from

$$n_{ef} = \frac{\phi - \phi_0}{k_0 l}. \tag{3}$$

In practice, ϕ_0 was set equal to $\phi|_{f\approx 7.84\text{ GHz}}$, which corresponds to the phase calculated at the frequency wherein the SPPs start propagating and the amplitude of the signal sensed by the receiving antenna becomes

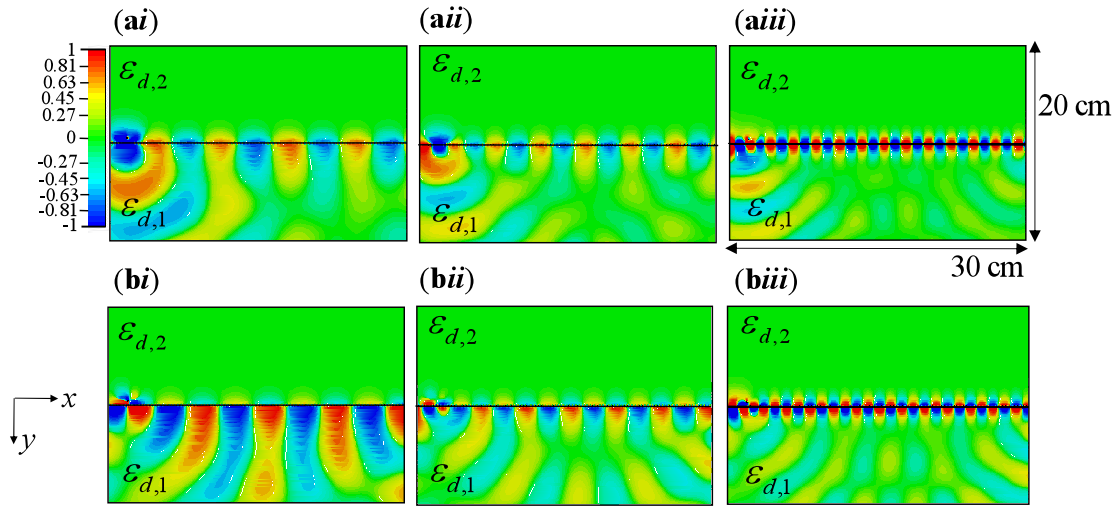

Figure 3. Numerically simulated field profiles of the SPPs supported by the waveguide-metamaterial prototype calculated at the mid-plane of the structure and for excitation of port 1. (a) Time snapshot of the transverse electric field component E_x. (ai) $f = 8.4$ GHz (aii) $f = 8.7$ GHz (aiii) $f = 8.9$ GHz. (b) Similar to (a) but for the normal electric field component E_y.

significant. The dispersion diagram measured using this method is depicted in figure 2(b) for the propagating distances $l = 18$ cm and $l = 10$ cm. As seen, there is a generically good agreement with the effective medium theory result (solid green line), especially for the longer propagating distance. The arms of the transmitting and the receiving dipoles have a finite length along the direction of the SPP propagation. This may cause an integrating effect on the phase of S_{ij} and some ambiguity in the definition of l, which is not accounted for in equation (3). Such finite-length 'correction' is less significant for larger values of l, which explains the better agreement in the $l = 18$ cm case. For comparison, we also provide in figure 2(a) the dispersion diagram obtained using the CST Microwave Studio® using the same extraction method (blue dashed and black dotted curves), for the same scenario as in the experiment, with the scattering coefficients S_{ij} obtained with a full wave numerical simulation. These diagrams have features analogous to the diagrams obtained with the experimental data in figure 2(b).

The electric field profile associated with the SPP waves was calculated using the CST Microwave Studio® (see figure 3) considering the same setup as in the experiment. Time snapshots of the electric field components E_x and E_y are represented in figures 3(a) and (b), respectively, for three different operating frequencies. As expected from the plasmon features, the surface wave is strongly confined at the interface between the two filling materials. Typical of the SPP propagation, the electric field components E_x and E_y decay exponentially in the direction orthogonal to the interface. As expected, E_y is flipped across the interface due to the different signs of the effective permittivity (figure 3(b)). Consistent with the dispersion diagram in figure 2, the guided wavelength is shorter for higher frequencies (figures 3(aiii) and (biii)).

The proposed paradigm enables extending the SPP concept to microwaves and terahertz frequencies and creates the conditions for the design of ultra-compact devices and waveguides. As an example, we consider an edge (Fabry–Pérot type) resonator formed by 34 wires, spanning length $L = 9.96$ cm (figure 4(a)). The resonator can be regarded as a truncated SPP waveguide. The resonance condition is given by $\beta_g L + \theta = m\,\pi$, where θ is the phase of the reflection coefficient of the SPP wave at the ends of the truncated waveguide, and $m = 1,\ 2,\ 3...$ labels the resonant mode [29]. Unfortunately, θ is not known analytically but it can be determined based on a numerical simulation. The resonance frequencies can be experimentally characterized by exciting the resonator with a small antenna (in our case the electric dipole located at $x_3 = 20$ cm) and by detecting the dips in the amplitude of the reflection coefficient ($|S_{33}|$). Figure 4(b) shows the plot of $|S_{33}|$ versus frequency, confirming the presence of several resonances. The difference between the experimental (blue curve) and the CST Microwave Studio® (green curve) results (e.g. the strength of the $m = 7$ resonance) is mainly due to the fabrication tolerances and the imperfect alignment of the dipole antenna. In addition, the microwave absorbers that surround the prototype are not ideal, and this causes that a few cavity modes (not related to the linear resonator) can be excited as well in the experiment. These cavity modes are usually associated with shallow dips in $|S_{33}|$ coefficient. Finally, it is important to keep in mind that only a few resonator modes are significantly excited by the antenna due to a mismatch between the field profiles and the antenna near field. The resonances that are better excited in the experiment occur for $f > 8.4$ GHz and are labeled with $m = 4,\ 5,\ 6,\ 9$ in figure 4(b). They match reasonably well the corresponding dips in the CST Microwave Studio® simulation. We numerically verified that these resonances are indeed resonator modes of order m. This is shown in figure 4(c), which represents a time snapshot of the electric field associated with each resonance. As seen, the fields are

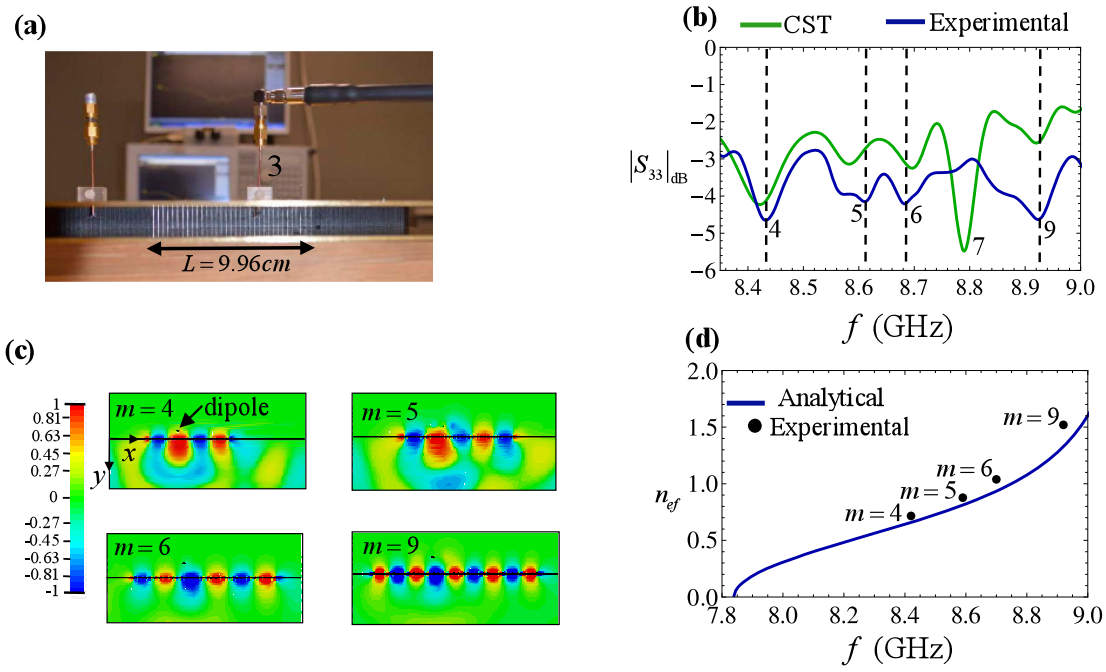

Figure 4. Edge resonator formed by a truncated SPP waveguide. (a) Photograph of the SPP resonator prototype formed by 34 metallic wires. (b) Amplitudes of the simulated and measured scattering parameter $|S_{33}|$ for an excitation (dipole 3) located at $x_3 = 20$ cm. The resonance frequencies of order $m = 4, 5, 6$ and 9 are marked in the plot. (c) Numerically simulated time snapshot of the electric field E_x for the resonance frequencies of order $m = 4, 5, 6$ and 9 (the area of the density plot may vary slightly from case to case). (d) Analytical dispersion diagram and experimental dispersion diagram points obtained from the reflection dips of figure 4(b).

associated with a standing wave with m lobes ($m + 1$ zeros). The dispersion diagram obtained with these four resonances (using $\beta_g L + \theta = m\,\pi$, and ignoring the phase θ, which is a reasonable approximation for a resonator with a significant number of wires, i.e. with a large L) is shown in figure 4(d). As seen, there is generically a good correspondence between the theoretical model and the experimental results obtained with the resonance frequencies of order $m = 4, 5, 6$ and 9, where the discrepancy is mainly related to the neglect of θ.

3. Conclusions

In summary, *single interface* plasmons have been experimentally verified at microwave frequencies through waveguide structures involving only conventional low loss positive-epsilon dielectrics. The metallic wires at the interface of the two dielectric regions guarantee the exclusive propagation of the TE_1 mode, and are the key to unlock the plasmonic effects using a waveguide-based metamaterial design. Full-wave numerical simulations and experimental measurements confirm the theoretical foundations of the equivalence between the proposed waveguide-metamaterial structure and an effective positive-ε medium paired with an effective negative-ε medium. Moreover, to illustrate the applications of the proposed paradigm we designed an edge Fabry–Pérot resonator formed by a truncated SPP waveguide. It is envisioned that this paradigm can have potential applications in the realization of microwave and terahertz plasmonic devices with low loss materials, particularly in systems where it is crucial to enhance light–matter interactions in a subwavelength scale. For example, if a subwavelength object is placed in the vicinity of the metamaterial interface, it will scatter strongly the SPP wave because of the short wavelengths of the wave. Thus, the proposed structure may find applications in sensing, spectroscopy, near-field imaging or even in free-electron lasers [30, 31].

Acknowledgments

This work was funded by Fundação para a Ciência e a Tecnologia under project PTDC/EEI-TEL/4543/2014 and by Instituto de Telecomunicações under project UID/EEA/50008/2013. F R Prudêncio acknowledges financial support by Fundação para a Ciência e a Tecnologia (FCT) under the Post-Doctoral fellowship SFRH/BPD/108823/2015. NE acknowledges partial support from the US Air Force Office of Scientific Research (AFOSR) Multidisciplinary University Research Initiatives (MURI) grant number FA9550-14-1-0389.

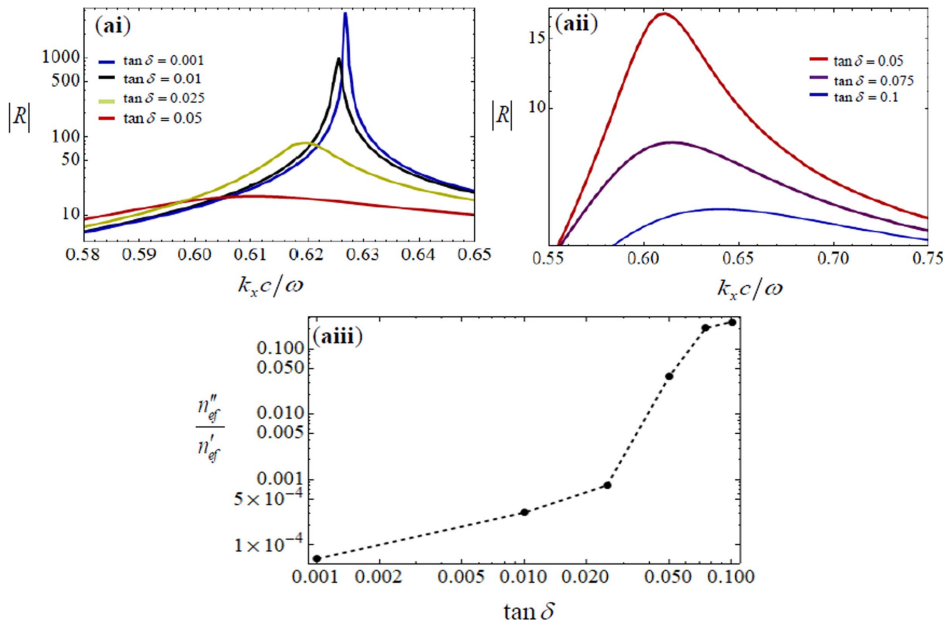

Figure A1. (ai), (aii) Amplitude of the reflection coefficient $|R|$ as a function of the wave number k_x of the incident wave for $f = 8.4$ GHz. The peaks are associated with the resonant excitation of the guided mode. The attenuation constant of the guided mode is determined by the quality factor of the resonance (−3 dB bandwidth). (aiii) Discrete symbols: calculated values of n''_{ef}/n'_{ef} as a function of the loss tangent of the dielectric (the symbols are joined with dotted lines to ease the interpretation of the data).

Appendix

In this appendix, we study the impact of dielectric and metal loss in the propagation constant of the SPPs. To this end, we numerically calculated for a fixed frequency the reflection coefficient R as a function of k_x when a TE_1 waveguide mode illuminates the interface between the two-waveguide regions in figure 1(b). Here, k_x is the (real-valued) wave number of the incident wave along x. For sufficiently large values of k_x the incident wave is evanescent, i.e., it decays along the y-direction perpendicular to the interface. When the value of k_x coincides with the propagation constant of a guided mode (β_g), the incident wave excites a natural mode of the system and in the absence of material loss $R \to \infty$. Thus, the guided modes are determined by the poles of $R(k_x)$. In the presence of loss, the poles become complex-valued, i.e., $\beta_g = \beta'_g + i\beta''_g$ is complex-valued. For weak loss, the reflection coefficient near the pole can be approximated by $R(k_x) = \dfrac{A}{(k_x - \beta_g)}$, so that

$$|R(k_x)| = \frac{|A|}{\sqrt{(k_x - \beta'_g)^2 + \beta''^2_g}}. \tag{A1}$$

The peak of R is attained at $k_x = \beta'_g$ and the −3 dB bandwidth of the resonance (when the amplitude of R is 70% of the maximum) is $(\delta k_x)_{-3dB} = 2\beta''_g$. From here it follows that:

$$\frac{n''_{ef}}{n'_{ef}} = \frac{\beta''_g}{\beta'_g} = \frac{(\delta k_x)_{-3dB}}{2\beta'_g} = \frac{k_{x2} - k_{x1}}{2\beta'_g}. \tag{A2}$$

In the above, $n_{ef} = n'_{ef} + in''_{ef}$ (with $n_{ef} = \beta_g/k_0$) is the guided effective refractive index, and k_{x2} (k_{x1}) is the value of k_x greater (less) than β'_g, such that the reflection coefficient $|R|$ is 70% of its maximum.

Figures A1(ai) and (aii) show the amplitude of the reflection coefficient $|R|$ plotted as a function of the normalized wave number of the incident wave, k_x, for dielectric substrates with $\tan\delta = 0.001$, $\tan\delta = 0.01$, $\tan\delta = 0.025$, $\tan\delta = 0.05$, $\tan\delta = 0.075$ and $\tan\delta = 0.1$, for $f = 8.4$ GHz. As expected, the quality factor of the resonance decreases as the loss is increased. Figure A1(aiii) shows the calculated n''_{ef}/n'_{ef}, obtained from the curves depicted in figures A1(ai) and (aii). As seen, for $\tan(\delta) < 0.01$ the effect of dielectric loss is insignificant. Furthermore, consistent with the theoretical estimate of the main text, the numerical results confirm that for small values of $\tan(\delta)$, n''_{ef}/n'_{ef} is proportional to $\tan(\delta)$, and at the considered frequency the proportionality constant is such that $n''_{ef}/n'_{ef} \approx 0.03 \tan\delta$.

We made a similar study to investigate the impact of metal loss on n''_{ef}/n'_{ef}, particularly at high frequencies. The methodology is the same as that described previously for the study of the dielectric loss. Figure A2(ai) shows the amplitude of the reflection coefficient $|R|$ a function of k_x, for different values of $\xi = \sigma/(\omega\,\varepsilon_0)$, σ being the

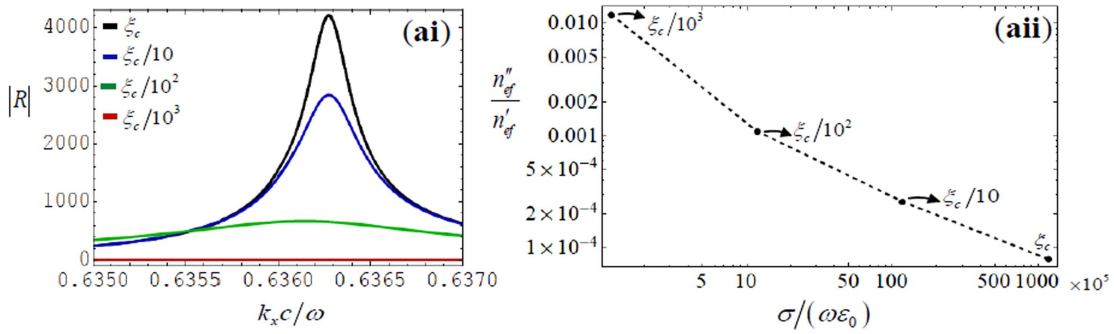

Figure A2. (ai) Amplitude of the reflection coefficient $|R|$ as a function of k_x for different values of $\xi = \sigma/(\omega\,\varepsilon_0)$. The case $\xi = \xi_c$ corresponds to the design of the article with the metal taken as copper and for an operation frequency of 8.4 GHz. (aii) Discrete symbols: calculated values of $n''_{\rm ef}/n'_{\rm ef}$ as a function of $\xi = \sigma/(\omega\,\varepsilon_0)$ (the symbols are joined with dotted lines ease the interpretation of the data).

conductivity of the metal and ε_0 the vacuum permittivity. We use normalized units so that $\omega a/c = 2.27$, $a_w/a = 0.23$ and $r_w/a_w = 0.1$, similar to the design discussed in the main text. For $\xi = \xi_c = \sigma_c/(\omega\,\varepsilon_0)$ with $\sigma_c = 5.9 \times 10^7$ S m^{-1} the copper conductivity, the parameters are as in the main text for an operational frequency of 8.4 GHz. The cases $\xi = \xi_c/10^i$ correspond to designs scaled to the working frequency 8.4 GHz $\times\ 10^i$ ($i = 1, 2, 3$), with the metal taken as copper. For simplicity, the metal conductivity is assumed frequency independent. As seen, in figure A2(aii) the proposed structure is fairly robust to the effect of metal loss, even for the designs operating at THz frequencies ($i = 2, 3$).

ORCID iDs

Filipa R Prudêncio https://orcid.org/0000-0002-7073-0987
Jorge R Costa https://orcid.org/0000-0002-1879-0026
Carlos A Fernandes https://orcid.org/0000-0001-5332-842X
Nader Engheta https://orcid.org/0000-0003-3219-9520
Mário G Silveirinha https://orcid.org/0000-0002-3730-1689

References

[1] Maier S A 2007 *Plasmonics: Fundamentals and Applications* (New York: Springer)
[2] Shvets G and Tsukerman I 2012 *Plasmonics and Plasmonic Metamaterials: Analysis and Applications* (Singapore: World Scientific)
[3] Cai W and Shalaev V 2007 *Optical Metamaterials—Fundamentals and Applications* (New York: Springer)
[4] Vakil A and Engheta N 2001 Transformation optics using graphene *Science* **332** 1291
[5] Engheta N 2007 Circuits with light at nanoscales optical nanocircuits inspired by metamaterials *Science* **317** 1698
[6] Pendry J B, Holden A J, Stewart W J and Youngs I 1996 Extremely low frequency plasmons in metallic mesostructures *Phys. Rev. Lett.* **76** 44773
[7] Pitarke J M, García-Vidal F J and Pendry J B 1998 Effective electronic response of a system of metallic cylinders *Phys. Rev.* B **57** 15261
[8] Belov P A, Marqués R, Maslovski S I, Nefedov I S, Silveirinha M G, Simovsky C R and Tretyakov S A 2003 Strong spatial dispersion in wire media in the very large wavelength limit *Phys. Rev.* B **67** 113103
[9] Silveirinha M G and Fernandes C A 2005 Homogenization of 3D- connected and non-connected wire metamaterials *IEEE Trans. Microw. Theory Tech.* **53** 1418
[10] Giovampaola C and Engheta N 2016 Plasmonics without negative dielectrics *Phys. Rev.* B **93** 195152
[11] Rotman W 1962 Plasma simulation by artificial dielectrics and parallel-plate media *IRE Trans. Antennas Propag.* **10** 82
[12] Silveirinha M G, Alù A and Engheta N 2007 Parallel-plate metamaterials for cloaking structures *Phys. Rev.* E **75** 036603
[13] Silveirinha M G, Alù A and Engheta N 2008 Infrared and optical invisibility cloak with plasmonic implants based on scattering cancellation *Phys. Rev.* B **78** 075107
[14] Silveirinha M G and Engheta N 2007 Design of matched zero-index metamaterials using nonmagnetic inclusions in epsilon-near-zero media *Phys. Rev.* B **75** 075119
[15] Alù A, Silveirinha M and Engheta N 2008 Transmission-line analysis of ε-near-zero-filled narrow channels *Phys. Rev.* E **78** 016604
[16] Marqués R, Martel J, Mesa F and Medina F 2002 Left-handed-media simulation and transmission of EM waves in subwavelength split-ring-resonator-loaded metallic waveguides *Phys. Rev. Lett.* **89** 183901
[17] Smith D R, Padilla W J, Vier D C, Nemat-Nasser S C and Schultz S 2000 Composite medium with simultaneously negative permeability and permittivity *Phys. Rev. Lett.* **84** 4184
[18] Esteban J, Camacho-Peñalosa C, Page J E, Martín-Guerrero T M and Márquez-Segura E 2005 Simulation of negative permittivity and negative permeability by means of evanescent waveguide modes—theory and experiment *IEEE Trans. Microwave Theory Tech.* **53** 1506
[19] Pendry J B, Martín-Moreno L and Garcia-Vidal F J 2004 Mimicking surface plasmons with structured surfaces *Science* **305** 847
[20] Hibbins A P, Evans B R and Sambles J R 2005 Experimental verification of designer surface plasmons *Science* **308** 670

[21] Maier S A *et al* 2006 Terahertz surface plasmon-polariton propagation and focusing on periodically corrugated metal wires *Phys. Rev. Lett.* **97** 176805
[22] Morgado T A, Marcos J, Silveirinha M G and Maslovski S 2011 Ultraconfined interlaced plasmons *Phys. Rev. Lett.* **107** 063903
[23] Demetriadou A and Pendry J B 2008 Taming spatial dispersion in wire metamaterial *J. Phys.: Condens. Matter* **20** 295222
[24] Luukkonen O, Silveirinha M G, Yakovlev A B, Simovski C R, Nefedov I S and Tretyakov S A 2009 Effects of spatial dispersion on reflection from mushroom-type artificial impedance surfaces *IEEE Trans. Microw. Theory Tech.* **57** 2692
[25] Maslovski S I and Silveirinha M G 2009 Nonlocal permittivity from a quasistatic model for a class of wire media *Phys. Rev.* B **80** 245101
[26] Li Y, Giovampaola C D and Engheta N 2016 Waveguide metatronics: lumped circuitry based on structural dispersion *Sci. Adv.* **2** 1501790
[27] Li Z, Liu L, Sun H, Sun Y, Gu C, Chen X, Liu Y and Luo Y 2017 Effective surface plasmon polaritons induced by modal dispersion in a waveguide *Phys. Rev. Appl.* **7** 044028
[28] GmbH C S T 2014 CST Microwave Studio http://cst.com
[29] Pozar M 1997 *Microwave Engineering* (New York: Wiley)
[30] Liu F, Xiau L, Ye Y, Wang M, Cui K, Feng X and Huang Y 2017 Integrated Cherenkov radiation emitter eliminating the electron velocity threshold *Nat. Photon.* **11** 289
[31] Silveirinha M G 2017 Low-energy Cherenkov glow *Nat. Photon.* **11** 269